UNIVERSITY OF BIRMINGHAM

The lodging of crops by tornadoes

Baker, Chris; Sterling, Mark; Jesson, Mike

[Link to publication on Research at Birmingham portal](#)

The lodging of crops by tornadoes

Chris Baker*, Mark Sterling, Mike Jesson

School of Engineering, University of Birmingham, Birmingham, United Kingdom

* corresponding author – c.j.baker@bham.ac.uk

Abstract

It is well known that tornadoes passing over fields can cause significant damage to crops, and tornado tracks of fallen, or lodged, crops can extend for many hundreds of metres. An examination of photographic evidence of such events suggests that, at least for low speed EF0 / EF1 events, lodging occurs beneath tornadoes primarily due to a strong radial flow (rather than circumferential flow) at the canopy surface. In order to investigate this effect further, a simple model of a tornado has been developed which, whilst fully satisfying the three dimensional Euler equations, models a circumferential flow at the edge of the tornado boundary layer near the ground, which becomes a radial flow as the ground is approached. This model is then used in a recently developed generalised model of lodging to predict lodging track widths and crop fall directions. It is shown that, when expressed in a suitably normalised form, both lodging width and crop fall direction are functions of a normalised translational velocity and a normalised crop lodging velocity. The lodging patterns are of two forms – a forward convergence (FC) where the cropfall converges on the tornado track in a forward direction, and a backward convergence (BC) where the convergence is in the opposite direction to tornado translations. Regions of FC and BC in the normalised parameter plane are calculated. These patterns are very similar to those observed

in the field, which gives some confidence in the nature of the model. The model is then used to investigate the sensitivity of lodging width to crop and tornado parameters, and also to carry out a risk analysis to determine the probability distributions of lodging width for specified distributions of crop and tornado parameters.

Notation

a	Crop stem radius (m)
AC_F	Crop drag area per plant (m^2)
f_n	Crop natural frequency (Hz)
F	Weibull PDF
g	Acceleration due to gravity (m/s^2)
k	Weibull shape parameter
K	Tornado parameter
P	Tornado pressure (Pa)
$\bar{P}$	$P/\rho V_m^2$
Q	Tornado translational velocity (m/s)
$\bar{Q}$	Q/V_m
$\widetilde{Q}$	$\bar{Q}/K$
r	Radial distance from centre of vortex (m)
r_m	Value of r at which circumferential velocity is a maximum (m)
$\bar{r}$	r/r_m
R	Asymmetry parameter
t	Crop wall thickness (m)
U	Tornado radial velocity (m/s)
U_m	Maximum value of U (m/s)
$\bar{U}$	U/V_m
V	Tornado circumferential velocity (m/s)
V_m	Maximum value of V (m/s)
$\bar{V}$	V/V_m
W	Tornado vertical velocity (m/s)

$\overline{W}$	W/V_m
x	Distance in tornado translation direction (m)
$\bar{x}$	x/r_m
X	Plant centre of gravity height (m)
y	Distance normal to tornado translation direction (m)
$\bar{y}$	y/r_m
z	Vertical distance above ground level (m)
z_m	Value of z at which circumferential velocity is a maximum (m)
$\bar{z}$	z/z_m
γ	Vortex constant
δ	z_m/r_m
Δ	Lodging width (m)
$\overline{\Delta}$	Δ/r_m
$\overline{\Delta}^*$	$\overline{\Delta}$ on positive side of convergence line
θ	Angle of radial flow from x direction (rad)
ϕ	Wind direction from x direction (rad)
λ	Weibull scale parameter
ρ	Density of air (kg/m^3)
σ	Crop stem strength (Pa)
ω_n	$2\pi f_n$ (rad/s)
Ω	Total wind velocity (m/s)
$\overline{\Omega}$	Ω/V_m
$\widetilde{\Omega}$	$\overline{\Omega}/K$
Ω_L	Lodging velocity (m/s)

$\overline{\Omega}_L$ $\qquad$ Ω_L/V_m

$\widetilde{\Omega}_L$ $\qquad$ $\overline{\Omega}_L/K$

1. Introduction

Lodging, the permanent displacement of cereal crops from the vertical due to the interaction of wind and/or rain, can affect yield loss, increase harvesting costs, reduce grain quality and decrease nutrient density (Berry et al., 2004). The cost of lodging can be considerable. For example, the combined costs of maize lodging in Mexico, Pakistan and China are estimated to be ~£600million every year (Berry, 2019). Thus, lodging has the potential to impact considerably on the economic development of countries and has a somewhat disproportionate effect on low and middle-income countries.

In general, there are two types of lodging: root lodging and stem lodging. The former occurs when the plant's displacement is due to failure at the root/soil interface, whilst the latter is due to failure of the plant's stem. A considerable degree of research has been undertaken into this phenomenon, mainly from an agricultural perspective (Pinthus, 1973; Neenan and Spencer-Smith, 1975; Thomas, 1982; Berry, 1998; Berry et al., 2000; White 1991; Fischer and Stapper, 1987 to name but a few). However, since 1995 a group of engineers and biologists have combined to tackle this multi-disciplinary challenge and have not only developed a model which correctly represents the physics of lodging process (Baker, 1995; Baker et al., 2014) but have also calibrated this model through field experiments relating to different crops (Sterling et al., 2003; Sterling et al., 2018). Perhaps not too surprisingly, attention has been focused on tropical or extra-tropical cyclones with a horizontal length scale of the order of 1000km, since these types of winds are generally considered to be responsible for the majority of lodging events. However, it has been recognized that non-cyclonic winds, in particular tornadoes, also cause both crop lodging and tree fall and that such

events can potentially be used as indicators of tornado wind speed – see Holland et al., (2006); Karstens et al., (2013); Lombardo et al., (2015); Rhee and Lombardo, (2018).

The tornado induced tree fall research studies have a number of points in common. They all use a tornado vortex model based on a translating Rankine vortex (i.e. forced vortex in the core, and free vortex outside the core). Usually a discontinuity in velocity gradient occurs where these two vortex formulations meet. Mechanical tree models of varying degrees of complexity are used that allow trunk breakage wind speeds to be determined, and tree fall directions are calculated as the tornado passes over an array of trees. Because trees are damaged or blown over at relatively high wind speeds, EF2 and EF3 tornadoes are usually considered in such analyses. In addition, the properties (mainly the height) of trees can be spatially variable, which will affect the breakage velocity in a spatially random way, and this has been allowed for in some models. These studies have revealed the basic tree fall patterns during tornado winds and have been compared with observed events.

Similar to the tree fall analysis outlined above, lodging in crops, particularly maize, has also been used to provide an insight into the strength of tornadoes, albeit to a lesser extent (Forbes and Wakimoto, 1982; Rhee and Lombardo, 2018). Such lodging will occur at significantly lower wind speeds (EF0 and below, i.e. less than 65mph / 30ms^{-1}). Whilst it is of interest to use maize damage tracks to estimate wind speeds, it is of less practical engineering use than is the case for trees, as EF0 tornadoes pose little risk to infrastructure. Such estimations may, however, be of considerable climatological interest. Potentially maize damage calculations could also be used to assess lodging risk and to thus estimate the potential yield losses,

and to assess what could be done to reduce these losses by changing plant mechanical and aerodynamic characteristics through appropriate breeding programmes.

The aim of this paper is thus to develop a model of the tornado lodging process which appropriately represents the physics of both tornadoes and lodging, and to use this model

- to investigate the relative importance of different crop agronomic parameters on the lodging process;
- to derive estimates of the probabilities of lodging risk, based on cumulative distribution functions of lodging track width;
- to investigate whether lodging track widths can be used to estimate near ground tornado velocities.

In section 2, we briefly outline the important aspects of the lodging model developed by Baker et al (2014). In Section 3 we then consider qualitative photographic evidence of tornado storm tracks through crops, which, it will be seen, gives insights into the type of tornado modelling required. Section 4 then sets out the tornado model that will be used. An overall tornado-lodging model is then developed in section 5 to predict lodging width, set out in a dimensionless format. This reveals the major parameters, and how the lodging patterns vary as these parameters change. Section 6 presents the results of a sensitivity analysis using this method to investigate how the various crop agronomic and tornado parameters affect lodging width. Section 7 then considers the calculation of lodging risk, and the results are briefly discussed and some concluding comments made in section 8.

2. The lodging model

In this paper we use the generalized lodging model of Baker et al., (2014). This models a field of crops as an array of vertical cantilevers with point masses representing the roots and the canopy. A fluctuating wind is considered to act on the top of the canopy and the resultant stem and root bending moments and displacements are calculated using conventional dynamic methods. Stem lodging is taken to occur when the stem bending moment exceeds the stem strength, and root lodging when the bending moment at the stem base exceeds the root / ground strength. The method requires that a range of crop, soil and meteorological parameters be specified. The model, and its predecessors, have been shown to reproduce the dynamic behaviour of a range of crops (Berry et al., 2003, 2004) and allowed the crop and soil parameters that most affect lodging to be identified. The model's ability to accurately assess the lodging behaviour of a range of crops has also been demonstrated.

Here we adapt the generalized model to the case of tornado lodging in two ways. Firstly, we assume that only stem lodging occurs. Stem lodging is caused by short-term wind gusts that cause stem bending moments to exceed the moments that lead to stem failure. Root lodging, by contrast has some aspects of a fatigue process and requires repeated oscillations of the crop / soil system over a period of several minutes. Short-term transient tornadoes are thus more likely to result in stem rather than root lodging. The assumption of stem lodging only is a significant simplification and removes the need for considering soil strength and rainfall rates and is in line with field observations where in general, stem lodging has been observed in tornado lodging events. Secondly, in Baker et al., (2014) the lodging velocities are expressed as hourly mean velocities. Here we express the stem

lodging velocities in tornadoes as a gust velocity, where the gust value is given by the tornado instantaneous wind speed. This wind speed should be interpreted as a short-term tornado wind speed of duration given approximately by the ratio of tornado radius to translational velocity. It will be seen in what follows that this ratio is of the order of unity, and thus the loading on the crop is effectively over a one second period – which is consistent with the formulation in Baker et al., (2014).

These assumptions lead to the following expression for (stem) lodging velocity Ω_L.

$$\Omega_L = \left(\frac{\omega_n^2 (X/g)(\sigma\pi a^3/4)\left(1-((a-t)/a)^4\right)}{\left(1+\omega_n^2(X/g)\right)(0.5\rho A C_F)} \right)^{0.5} \tag{1}$$

Here ω_n is the radial natural frequency of the crop ($= 2\pi f_n$) where f_n is the actual natural frequency; X is the crop centre of gravity height above ground; g is the acceleration due to gravity; σ is the stem bending strength; a is the stem radius; t is the stem wall thickness; ρ is the density of air (=1.22 kgm^{-3}); and AC_F is the plant drag area. The lodging model thus considers failure to occur in individual stems. However the model itself is based on a whole canopy where the plants may or may not interact strongly with each other with this interaction represented indirectly through the natural frequency and damping ratios used in the model.

Values of all the crop parameters for maize have been measured in the recent experimental campaigns reported by Sterling et al., (2018), and typical in-field means and standard deviations for the various parameters are shown in table 1 below. These parameters have been obtained under UK conditions, and can be expected to vary for different regions and climates. We will use the mean values of these parameters in table 1 as the "base case" for parametric investigations

described below. From equation (1) above these give a base case lodging velocity of 12.5m/s.

	Mean	Standard deviation
f_n (Hz)	0.7	0.12
X (m)	0.95	0.1
σ (MPa)	21.9	4
a (m)	0.013	0.0013
t (m)	0.0026	0.0005
AC_F (m²)	0.163	0.02

Table 1 Crop parameters for maize

3. Observations of lodging

Before proceeding to develop an analytical framework to consider crop lodging due to tornadoes, it is worthwhile to consider some visual observations of the lodging process. Figure 1 shows two photographs of recent events, together with an interpretation of the crop fall directions. It is immediately obvious that the predominant pattern is one that appears to show crop fall converging on the centre of the tornado track, and has no relationship to the direction of the crop rows. In the case of figure 1a the pattern seems to be a convergence of lodging direction in the direction of tornado translation, whilst in figure 1b it seems to be a convergence in the opposite direction. This is at first sight somewhat odd, since a simple consideration of lodging due to the swirling flow in a tornado would lead one to expect at least some lodging perpendicular to the storm track near to the tornado centre. These observations, and other similar ones, strongly suggest that lodging occurs primarily due to some combination of the tornado translational velocity and a radial flow within the vortex core. This has significant implications

for modelling the process. The majority of analytical tornado models are essentially two dimensional and based on a Rankine vortex formulation, without allowance for either radial flows or variation with height. The model recently developed by Baker and Sterling (2017) and used in the analyses of Baker and Sterling (2018a, 2018b) allows for tornado velocities in circumferential, radial and vertical directions. This model still, however, has its limitations – the vertical velocity component is not bound and increases monotonically with height, and the circumferential and radial flows fall to zero at the ground. For the current application, some velocity component near the ground is required, although the fact that crop canopies are porous and deflect significantly in the wind makes it difficult to define the effective ground level with any accuracy.

Thus in what follows we develop a new model, and it will be seen that this possesses the normal swirl characteristics of tornadoes away from the ground, but the circumferential and vertical components fall as the ground is approached, leaving only a radial flow. The model is theoretically sound, being consistent with the three dimensional Euler equations, and offers a way in which the strength of the radial flow at the surface can be related to the above surface flow characteristics.

Whether or not such a radial flow exists beneath tornadoes at ground level in general (i.e. not just above crops) is difficult to judge. The results of Rhee et al (2018) and Chen and Lombardo (2019) for tree fall seem to indicate that this occurs, in the main, due to the expected swirling flow, and the treefall direction is mainly across the tornado track, although the loading on trees will be caused by wind conditions several metres above the ground. This point will be considered further below in section 5.

Finally it is worth making a comment with regard to lodging track length. There is little data available on this, but what there is suggests it is highly variable. National Weather Service (2016), in a study of 111 tornado tracks, found track lengths of between 130m and 18km. Whilst this is not of relevance to the calculations of lodging width reported here, it could be of importance in calculating wide scale lodging risk. This point will be considered further below.
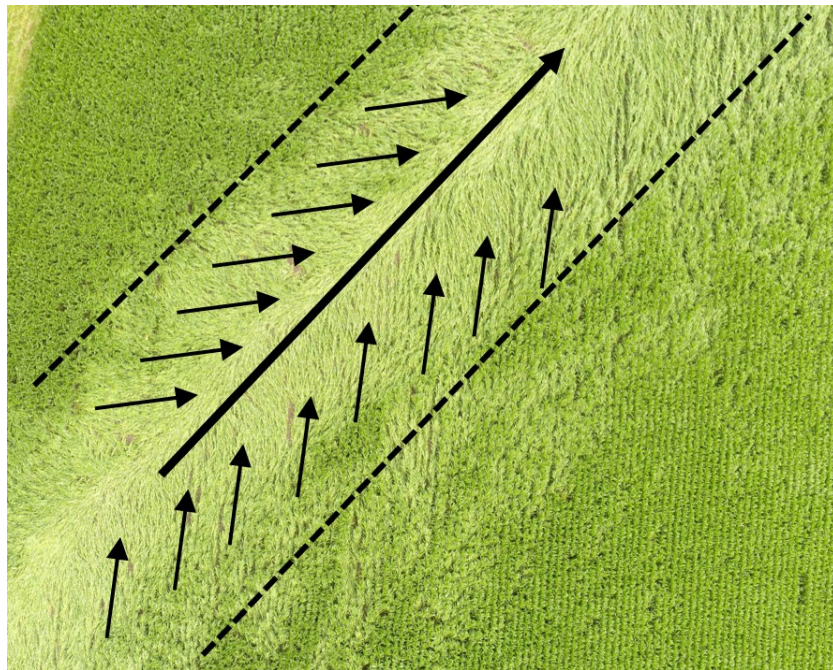
(a) Rantoul, IL tornado 2018 (from Frank Lombardo, UIUC)
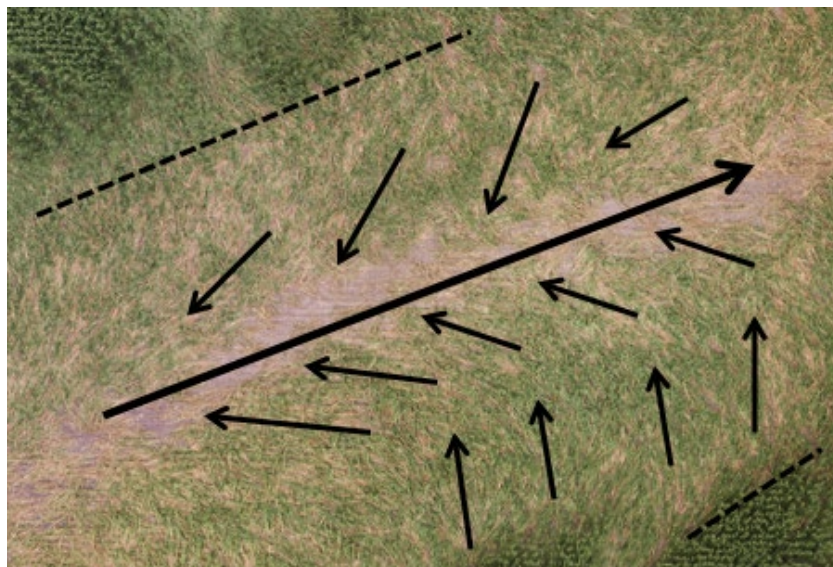
(b) Bondurant, IL tornado in 2018. (from Todd Rector

https://www.facebook.com/StormChaserTodd/posts/268639840386352)

Figure 1 Observed lodging directions (short arrows indicate lodging direction, long arrows indicate tornado translation direction, dotted lines show approximate extent of lodged area)

4. Tornado wind field

The tornado model that will be used in this paper is set out in Appendix 1. It begins with the assumption of a form for circumferential velocity that has a maximum value at the edge of the tornado boundary layer and falls to zero at the ground. This form is then used in the continuity and momentum equations to obtain values of the radial and vertical velocities and pressure that are consistent with the Euler equations. Essentially a single cell vortex is modeled. Full scale experiments suggest that such a model is a good representation of fairly low intensity tornadoes of relevance to the lodging issue (National Weather Service, 2016). As the tornado wind speeds increase, multiple cell vortices become more common, but the wind speeds in such tornadoes are much higher than would cause the relatively restricted lodging tracks considered here. The velocity components are given by

$$\bar{U} = -K \frac{\bar{r}}{(1+\bar{r}^2)} \frac{(1-\bar{z}^2)}{(1+\bar{z}^2)^2} \tag{2}$$

$$\bar{V} = \frac{4\bar{r}\bar{z}}{(1+\bar{r}^2)(1+\bar{z}^2)} \tag{3}$$

$$\bar{W} = \delta K \frac{2}{(1+\bar{r}^2)^2} \frac{\bar{z}}{(1+\bar{z}^2)} \tag{4}$$

$\bar{U} = U/V_m$, $\bar{V} = V/V_m$, and $\bar{W} = W/V_m$, where U, V and W are the radial, circumferential and vertical velocities and V_m is the maximum value of V. $\bar{r} = r/r_m$ and $\bar{z} = z/z_m$ where r and z are the radial distance from the vortex centre and height above ground respectively and $\delta = z_m/r_m$. $V = V_m$ at $r = r_m$ and $z = z_m$. K is a constant of integration that is proportional to the ratio of the maximum radial velocity to the maximum circumferential velocity.

At ground level the circumferential and vertical velocities fall to zero. The radial velocity however becomes

$$\bar{U} = -K\frac{\bar{r}}{(1+\bar{r}^2)} \tag{5}$$

From equation (5) the maximum radial velocity $U_m = V_m K/2$ when $\bar{r} = 1$. The utility of this particular model is that it relates, through a self-consistent formulation, a strong inflow at ground level with a swirling flow above the ground – which is precisely what the somewhat limited results of figure 1 suggest is required.

Now for the case of a translating vortex, we assume that the translating tornado produces only a radial velocity U at ground level, positive outwards from the centre of the tornado vortex. It is translated at a speed Q in the x direction. The velocity at a point (x, y) relative to the centre of the tornado vortex is given by the vector sum of these velocities (figure 2). In this figure r is the radial distance from the vortex core $(x^2 + y^2)^{0.5}$, and θ is the angle of the radial velocity to the x-axis. From figure 2, the following equations can be derived for the magnitude of the overall normalised tornado velocity at ground level, $\bar{\Omega} = \Omega/V_m$, and its direction ϕ.

$$\bar{\Omega} = ((\bar{Q} + \bar{U}\cos\theta)^2 + (\bar{U}\sin\theta)^2)^{0.5} \tag{6}$$

$$\tan\phi = \frac{\bar{U}\sin\theta}{\bar{Q}+\bar{U}\cos\theta} \tag{7}$$

where $\bar{Q} = Q/V_m$ is the normalised tornado translational velocity. Using the definition of radial velocity component given above, these result in the expressions

$$\bar{\Omega} = \left(\bar{Q}^2 + \frac{(\bar{x}^2+\bar{y}^2)K^2}{(1+\bar{x}^2+\bar{y}^2)^2} - \frac{2\bar{Q}\,K\bar{x}}{(1+\bar{x}^2+\bar{y}^2)}\right)^{0.5} \tag{8}$$

$$\phi = \text{atan}\left(\frac{-K\bar{y}}{\bar{Q}(1+\bar{x}^2+\bar{y}^2)-K\bar{x}}\right) \tag{9}$$

These two equations can be further simplified by letting

$$\widetilde{\Omega} = \frac{\overline{\Omega}}{K} \tag{10}$$

$$\widetilde{Q} = \frac{\overline{Q}}{K} \tag{11}$$

then equations (8) and (9) can be written

$$\widetilde{\Omega} = \left(\widetilde{Q}^2 + \frac{(\bar{x}^2 + \bar{y}^2)}{(1 + \bar{x}^2 + \bar{y}^2)^2} - \widetilde{Q}\frac{2\bar{x}}{(1 + \bar{x}^2 + \bar{y}^2)}\right)^{0.5} \tag{12}$$

$$\phi = \mathrm{atan}\left(\frac{-\bar{y}}{\widetilde{Q}(1 + \bar{x}^2 + \bar{y}^2) - \bar{x}}\right) \tag{13}$$

Thus the tornado velocities and flow directions can be represented as functions of the dimensionless position relative to the vortex centre and just one other variable – the normalised translational velocity $\widetilde{Q}$.
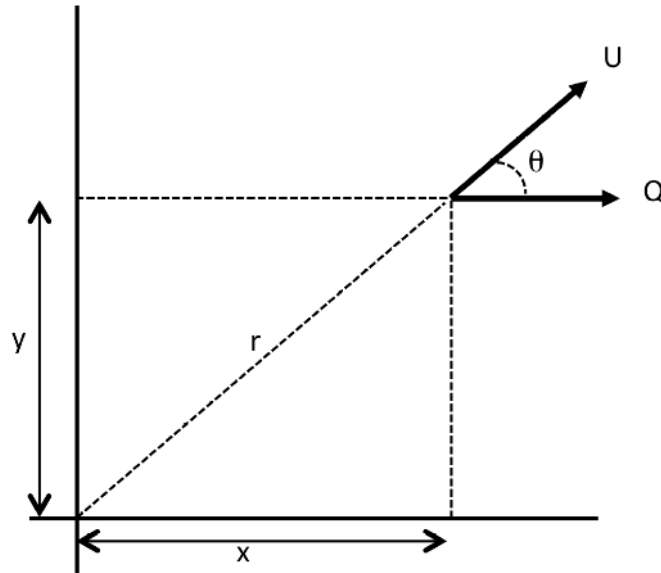

Figure 2 Tornado velocity vectors.

5. Lodging track width and lodging direction

In this section we will apply the method outlined in the last section to calculate what we will describe as the lodging width. This is defined as the width of crop that is lodged, perpendicular to the lodging direction, as the tornado passes over it (Δ). We assume that the crop will lodge at the point where the resultant tornado velocity first exceeds the stem lodging velocity. It can be expected that lodging will occur at different lateral distances from the vortex track for different distances along the track from the vortex centre. From equations (12) and (13) above, the dimensionless lodging track width perpendicular to the tornado translational direction is given by

$$\overline{\Delta} = \frac{\Delta}{r_m} = function\left(\widetilde{\Omega}_L, \widetilde{Q}\right) \tag{14}$$

where $\widetilde{\Omega}_L = \overline{\Omega}_L/K$, $\overline{\Omega}_L = \Omega_L/V_m$ and Ω_L is the dimensional wind speed at which lodging occurs. The functional form is algebraically complicated (although simple in principle) and is best calculated numerically. Figure 3 shows the results of such a calculation for $\widetilde{\Omega}_L$ = 0.5 and $\widetilde{Q}$ = 0.15. Figure 3a shows the maximum value of $\widetilde{\Omega}$ on any $\overline{y}$ section - lodging will occur if $\widetilde{\Omega}$ exceeds $\widetilde{\Omega}_L$. For this case, the dimensionless lodging width $\overline{\Delta}$ is 3.3. Figure 3b shows the lodging front i.e. the position relative to the centre of the vortex where lodging will first occur. It can be seen that this is quite complicated in shape, with lodging first occurring near the edge of the vortex core before the vortex centre arrives, and in the centre of the vortex track after the centre of the vortex has gone by. Figures 3c and 3d show, in different ways, the lodging direction i.e. the direction in which the crop will fall. In figure 3c the lodging angle is 0° in the direction of tornado translation and ±180° in the direction opposite to tornado translation. Figures 3c and 3d indicate

a forward convergence (FC) of lodging direction towards the centre line of the tornado track, with the directions converging on $\pm 0°$ as $\bar{y}$ goes to zero. At the centre line lodging occurs just after the vortex centre has passed, when the sum of the vortex inflow velocity and the translational velocity, which are acting in the same direction, exceeds the lodging velocity. This results in the crops in this region falling in the direction of tornado translation - which compares favourably with the directions shown in figure 1a.

Now consider the case of figures 3e to 3h where $\widetilde{\Omega}_L = 0.30$, and $\widetilde{Q} = 0.15$. For these values the convergence towards the centre line is in the opposite direction to the base case – a backwards convergence (BC), with the directions converging on $\pm 180°$ as $\bar{y}$ goes to zero. This is because in this case the lodging front is ahead of the vortex centre line, the vortex inflow velocity is in the opposite direction to the tornado translation velocity, and lodging occurs when the difference between these velocities exceeds the lodging velocity. The lodging direction is in accord with the lodging directions given in figure 1b. There is however a slight asymmetry in figure 1b that is not reproduced in figures 3e to 3h.

Lodging patterns very similar to those of figure 3 have also been predicted using the Rankine flow model with arbitrary radial inflow of Rhee and Lombardo (2018), for the cases where they allow radial flows to dominate.

Figure 4 shows the variation of lodging width $\bar{\Delta}$ in the $\widetilde{\Omega}_L$- $\widetilde{Q}$ plane. Regions of no lodging NL, FC and BC can be defined in this plane. From equations (5) and (6) at $\bar{r} = 1$ on the x axis and the definitions of equations (10) and (11) the boundary between NL and FC is given by

$$\widetilde{\Omega}_L = 0.5 + \widetilde{Q} \tag{15}$$

and the boundary between FC and BC is

$$\widetilde{\Omega}_L = 0.5 - \widetilde{Q} \qquad\qquad (16)$$

The positions of the cases shown in figure 3 are shown in figure 4 and can be seen to be in the FC and BC regions respectively. In general $\overline{\Delta}$ increases as $\widetilde{Q}$ increases and as $\widetilde{\Omega}_L$ decreases. The variations in $\overline{\Delta}$ show no discontinuity across the FC / BC boundary.

In principle it should be possible to locate the two tornadoes of figure 1 the $\widetilde{\Omega}_L$- $\widetilde{Q}$ plane in figure 4. For both tornadoes, data on track width and length, duration and speed is available from National Weather Service (2018a,b). There is considerable uncertainty in these data as the wind speeds in the tornadoes can only be specified from the EF damage indicators and thus have a wide range. In addition there is no direct measurement of lodging velocity. The best that can be said, assuming that the lodging velocity is around the base case (UK) value, is that both tornadoes sit around the FC / BC boundary in the bottom right of figure 4, with values of both $\widetilde{Q}$ and $\widetilde{\Omega}_L$ of around 0.25 to 0.30.

Figure 5 shows the variation of lodging direction with both variations in $\widetilde{Q}$ (figure 5a) and $\widetilde{\Omega}_L$ (figure 5b) around the base case. Note the scales on these two figures are different. It can be seen that as $\widetilde{Q}$ varies the pattern of lodging directions remains the same with a convergence on ±0° as $\overline{y}$ goes to zero i.e. all of the FC type. As $\widetilde{\Omega}_L$ varies, however, there can be seen to be a smooth transition from FC to BC between values of $\widetilde{\Omega}_L$ between 0.3 and 0.4, with the latter displaying a convergence to ±180° as $\overline{y}$ goes to zero.

Before moving on to consider applications of the combined tornado / lodging model, it is worth considering the tornado model in a little more detail. In this paper, it has been formulated at ground level, in order to model the radial inflow that seems to cause lodging in crops. However, equations (2) and (3) can be used

to specify tornado velocities at different heights above the ground. At $\bar{z} = 1$ the flow is wholly circumferential, with the velocity at intermediate heights having both radial and circumferential components. It is shown in Appendix 2 that the lodging directions predicted using the velocity for heights between $\bar{z} = 0.05$ and $\bar{z} = 0.5$ show a similar asymmetry to that seen in figure 1b, and the lodging patterns using the velocity for heights between $\bar{z} = 0.05$ and $\bar{z} = 0.5$ are very similar to those for trees observed in Rhee and Lombardo (2018) and Chen and Lombardo (2019), with lodging across the direction of travel, but with an off centre line of convergence. The implication of this is that velocities around $\bar{z} = 0.5$ *to* 1 are responsible for tree fall, and thus, since this height is at the edge of the tornado boundary layer, the boundary layer thickness is of the order of tree height – perhaps 4 to 8m in thickness.
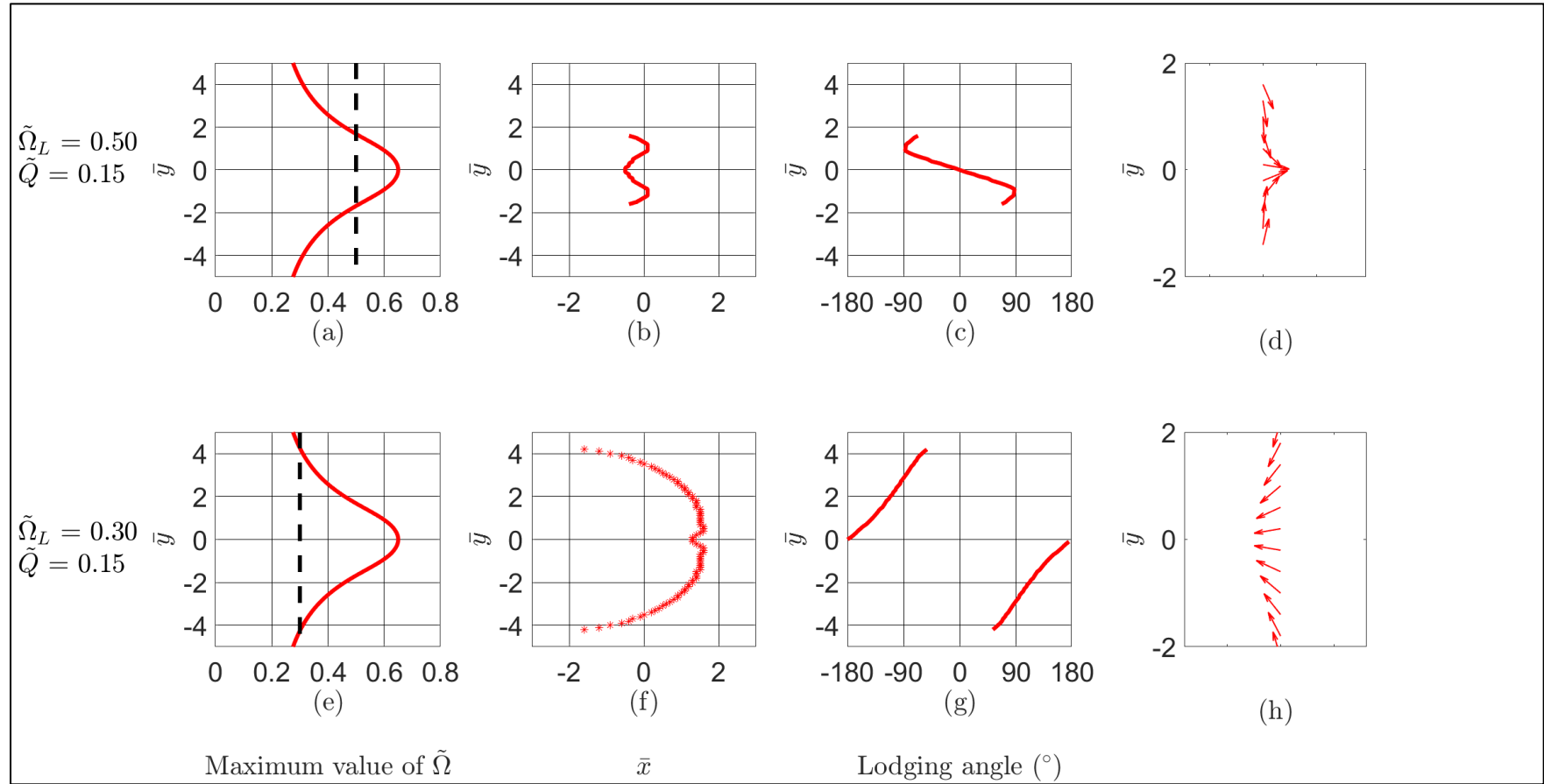
Figure 3 Tornado lodging model calculations

((a) and (e) show the maximum velocity on any $\bar{y}$ section with the dotted line showing $\widetilde{\Omega}_L$; (b) and (f) show the lodging front; (c) and (g) show the lodging directions in graph form; (d) and (g) show the lodging directions in vector form)
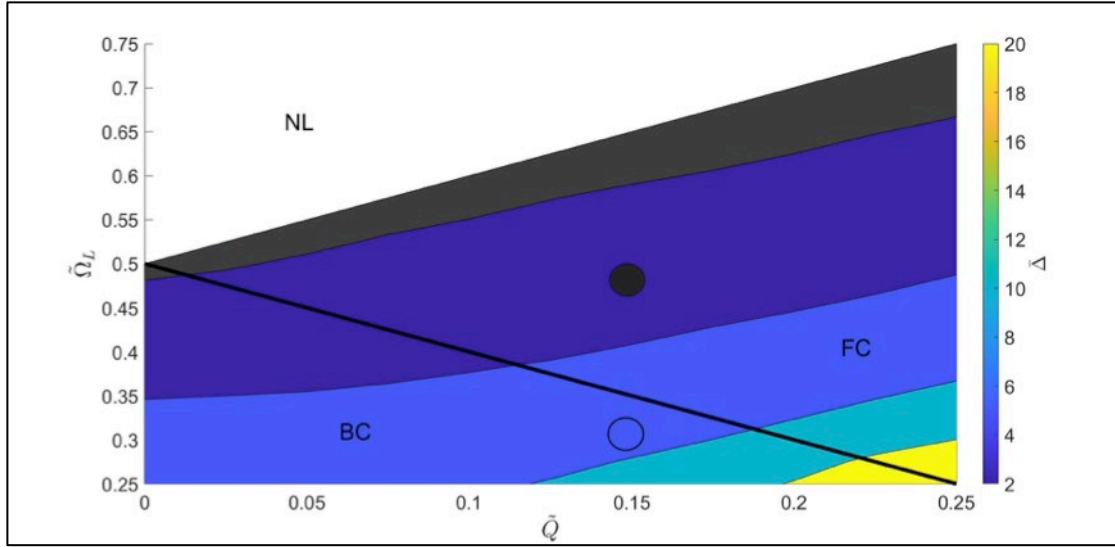
Figure 4 Contours of $\overline{\Delta}$ in the $\widetilde{\Omega}_L$ - $\widetilde{Q}$ plane

(FC- Forward Convergence, BC – Backward convergence, NL – no lodging, Filled

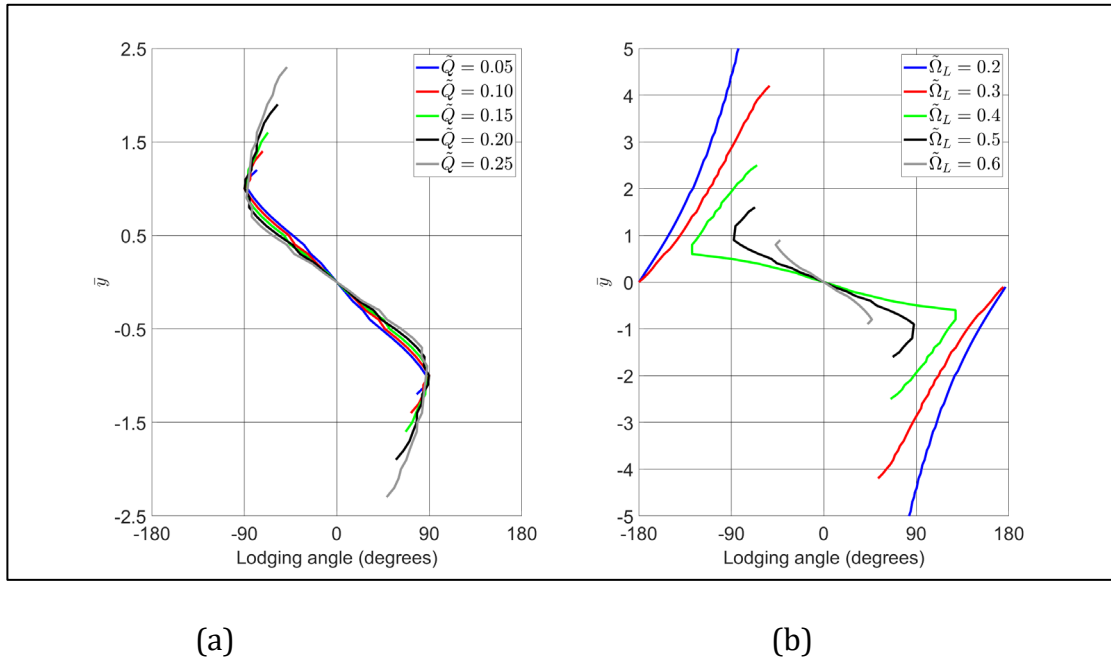circle – $\widetilde{\Omega}_L = 0.5$ and $\widetilde{Q} = 0.15$, open circle $\widetilde{\Omega}_L = 0.3$ and $\widetilde{Q} = 0.15$)

(a)   (b)

Figure 5 Variation of lodging direction with variations in $\widetilde{Q}$ and $\widetilde{\Omega}_L$

6. Sensitivity analysis

The dimensionless analysis outlined in the last section is useful in describing in a succinct way the overall nature of the problem, and the relationships between the different lodging patterns that have been observed in the field. In practical terms however, it is necessary to work in dimensional terms to obtain real, as opposed to normalised, values of lodging width. To do so we need to define the maximum circumferential velocity V_m, the parameter K, the translational velocity Q and the lodging velocity Ω_L. In what follows we will define a base case and calculate the lodging width for that set of parameters, then vary the parameters around the base case values to assess the sensitivity of the calculations. For the base case

- V_m = 25 m/s, which represents an EF0 tornado;

- K = 1;

- Q = 3.75 m/s;

- Ω_L=12.5m/s (see section 2).

The values of V_m and K give a value of U_m = 12.5 m/s. The dimensionless parameters of the last section have values of $\widetilde{Q}$ = 0.15 and $\widetilde{\Omega}_L$ = 0.5 i.e. the same as those used for the calculations of figure 3a to 3d.

The vortex core radius r_m is also required, as it is used to normalize all length scales. For this, we use the work of Fan and Pang (2019) who provide data for r_m for a range of EF scale values. For the lower EF values a straight line fit to the data can be derived as follows

$$r_m = 7.0725 \left(\left(\frac{V_m}{15.6} \right) - 1 \right) \tag{17}$$

for 15.6m/s < V_m < 50m/s, and a zero value for lower values of V_m. For the base case, the value of r_m is 4.3m.

Table 2 shows the calculated lodging width for variations of the four velocities about the base case. Variations in Q represent movement along a $\widetilde{\Omega}_L=$ constant line in figure 4 and variations in Ω_L represent movement along a $\widetilde{Q}=$ constant line. Variations of U_m result in both variations to $\widetilde{Q}$ and $\widetilde{\Omega}_L$. Variations in V_m affect the results through variations in the vortex core radius. Broadly, it can be seen that, for the parameter range considered variations in V_m and Ω_L are of most significance.

Variations in the latter are of course caused by variations in the crop parameters, and table 3 shows how Ω_L varies as the crop parameters vary between (mean $\pm$ 2 x standard deviation), with the means and standard deviations as given in table 1. It can be seen that Ω_L increases as the centre of gravity height and drag area decrease and as natural frequency, stem strength, stem diameter and stem wall thickness increase, all of these effects being physically reasonable. The variations are nearly all within the 10 to 15m/s assumed in table 2. The values are most sensitive to variations in stem strength, stem radius and drag area. This does not of course take into account variations in multiple parameters at one time.

Table 2 Calculated lodging widths

(Note that variations in U_m imply a variation in the parameter K)

V_m (m/s)	20	25	30		25			25			25	
U_m (m/s)		12.5		10	12.5	15		12.5			12.5	
Q (m/s)		3.75			3.75		2.5	3.75	5.0		3.75	
Ω_L (m/s)		12.5			12.5			12.5		10	12.5	15
Δ (m)	6.6	14.1	21.6	8.1	14.1	19.2	12.4	14.1	16.6	21.8	14.1	8.1

Table 3 Sensitivity of Ω_L to crop parameters

(Values in m/s)

	Mean – 2 x standard deviation	Mean	Mean + 2 x standard deviation
f_n (Hz)	10.4	12.5	13.6
X (m)	13.5	12.5	12.1
σ (MPa)	10.0	12.5	14.6
a (m)	9.6	12.5	15.4
t (m)	10.4	12.5	13.9
AC_F (m^2)	14.4	12.5	11.2

7. Calculation of lodging risk

The methodology of this paper can also be used to obtain a quantitative estimate of lodging risk (and thus of yield loss). This involves creating a large ensemble of random realisations of the crop and tornado parameters, and calculating the lodging width for each realization. A probability distribution functions (PDF) and a cumulative distribution function (CDF) of lodging width can then be derived, which will show the probability of a specific lodging width being exceeded. This can then be combined with the probability of a tornado occurring at a particular location (usually of the order of 10^{-5} per annum per km^2) to obtain the overall risk of a particular lodging width.

Now it is known that the probability of tornado wind speeds is given by a Weibull distribution (Dotzeka ,., 2003) with a PDF given by

$$F = \left(\frac{k}{\lambda}\right)\left(\frac{V_m}{\lambda}\right)^{k-1} e^{-\left(\frac{V_m}{\lambda}\right)^k} \tag{18}$$

where λ is a scale parameter, and k is a shape parameter. Dotzeka et al., (2003) give values of these parameters for a wide variety of geographical locations. The scale parameter simply moves the distribution along the velocity axis as it is changed. The shape parameter however has a more marked effect and is known to vary widely from country to country. Dotzeka et al. give values of k of around 1.5 to 3.0 for the USA, 1.0 in Argentina, 2.0 in Australia and close to 4 in the UK. A low value of k indicates a very wide spread of tornado wind speeds, including very high values, while a high value of k indicates that the extreme values of tornado wind speeds do not occur. Figure 6 shows the PDFs for shape parameters of 1, 2 and 4 for scale parameters that keep the median of the distribution at 25m/s. For k=1 equation (18) becomes an exponential distribution which shows the highest

probabilities in both the low and high tornado wind speed ranges. At the other end of the range, for *k*=4, there can be seen to be a peak in probabilities in the mid speed range. The probabilities for *k*=2 (a Rayleigh distribution) are intermediate between the two extreme cases.
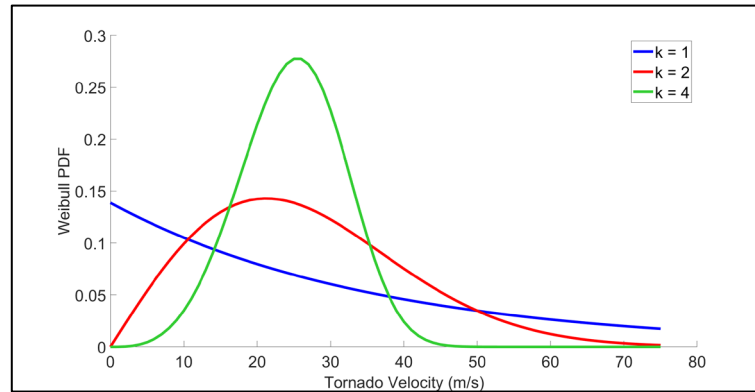

Figure 6 Variation of Weibull distributions with shape parameter

The use of the Weibull distribution to generate tornado wind speeds for this particular application is not wholly straightforward. For values of shape parameter less than 3 to 4, the generated velocities will include very low values and very high values. The former are unrealistic, whilst the latter imply strong tornadoes, where whole areas of crop would lodge – which is not really the case under consideration here, and for which the tornado parameterisation does not apply. Thus, in what follows we use a value of *k* of 4.0, which is applicable for all tornadoes in a country such as the UK, where maximum speeds are low, but for other countries, such as the USA, should be interpreted as only applying to EF0 to EF2 tornadoes. In the latter case the overall probability of a tornado occurring should be that for tornadoes of EF2 and less.

The crop parameters were assumed to be normally distributed with the means and standard deviations of table 1. 5000 parameter realisations for tornado and crop parameters were used, in which tornado and crop properties were generated

28

randomly based on the assumed probability distributions. We assume that the maximum radial velocity and the translational velocity are the values for the base case at V_m =25m/s, and vary linearly with V_m i.e. they are not treated as independent stochastic variables, and K and $\tilde{Q}$ are constant.

Figure 7 shows the PDFs for the simulated wind speeds and lodging widths using a Weibull scale parameter of 27.4m/s and shape parameter of 4.0, which has a median value of 25m/s and is thus consistent with the base case of the last section. The simulated windspeed distribution is compared with the target values directly calculated from the Weibull distribution, and the results of the simulation can thus be seen to be close to the target distribution. The PDF for lodging risk shows that 12% of realisations produce no lodging (either due to low wind simulated wind speeds, or strong crops). For those realisations where lodging occurs, probabilities decrease with increases of lodging width as expected.

The resulting CDF for lodging width is shown in figure 8 and allows the probability that the lodging width exceeds a certain value to be calculated. Whilst the median (50%) value is 17.4m, it can be seen that around 12% of realisations produce very large lodging widths >100m.

Figure 9a shows, for the same parameters, a plot of all the realisations of lodging width against the corresponding tornado velocities. Note the point made in section 2 concerning the nature of the tornado model. It is of the single cell type that is not really applicable to the higher wind speeds shown in this figure. The lodging width can be seen to be quite a strong function of the tornado velocity, as might be expected, with the scatter around the mean illustrating the variability of the crop agronomic parameters. The means and standard deviations of these realisations for different velocity bands are shown in figure 9b. These results

suggest that if crop characteristics are known, the lodging width may be used to give at least a broad indication of maximum tornado velocities (and the associated uncertainties inherent with such velocities).
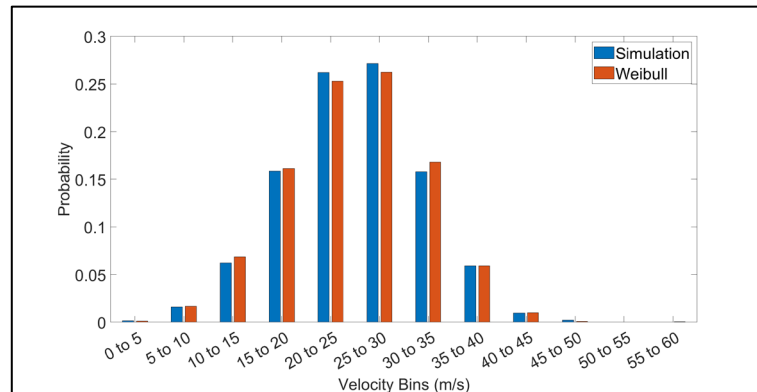
a) PDF of simulated and target wind speed distribution
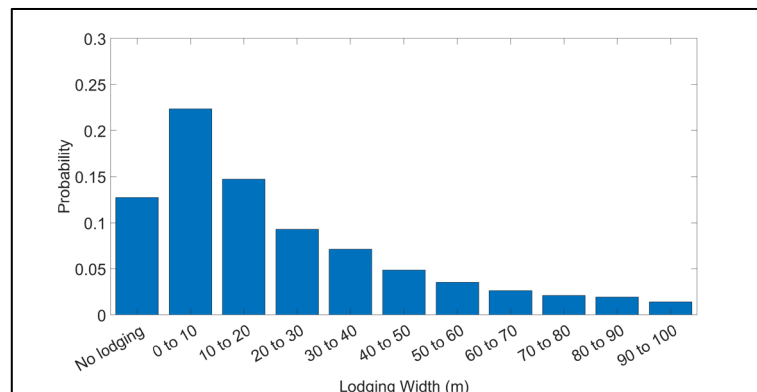
b) PDF of lodging widths
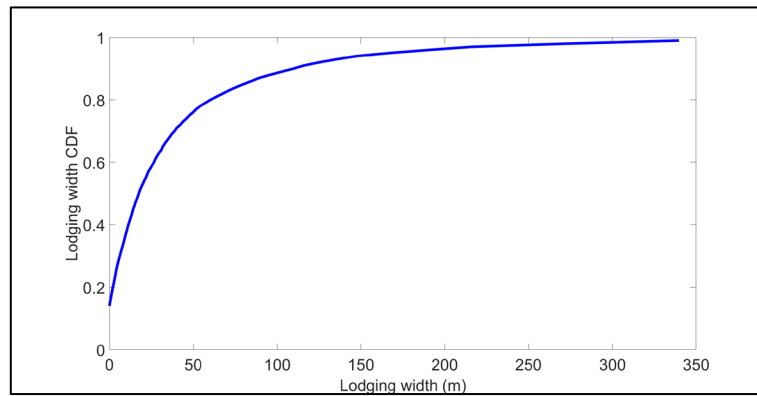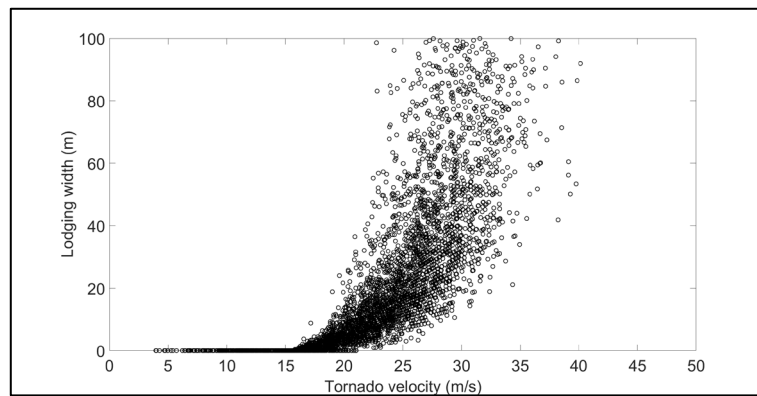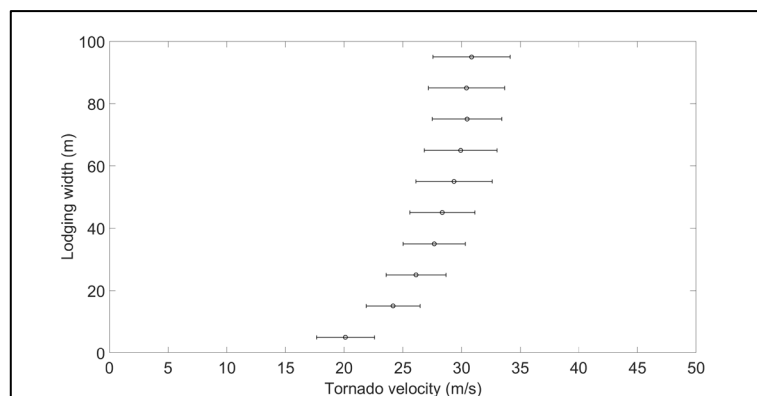
Figure 7 Simulated PDFS of wind speed and lodging risk

Figure 8 CDF of lodging width

(a)

(b)

Figure 9 Lodging width against tornado velocity for individual realisations

8. Conclusions

This paper has outlined a methodology to describe the lodging of crops during tornadoes. The following major conclusions can be drawn.

- A study of images of crop lodging beneath tornadoes suggests that lodging is primarily driven by a radial inflow close to the top of the crop – in other words the circumferential velocity in the tornado falls to close to zero near the ground. This may be a general feature of small tornadoes close to ground level, or it might be caused by an interaction between the tornado and the crop.

- An analytical model has been developed, based on the three dimensional Euler equations that begins with the assumption the circumferential velocity falls to zero near ground level, and results in an expression for radial velocity that has a finite value at ground level.

- This model is then used in conjunction with a proven generalized lodging model, and is shown to be able to predict lodging directions that are consistent with the photographic evidence, in that converging / diverging lodging patterns are predicted. It also allows the effects of tornado parameters on lodging patterns to be investigated and regions of forward convergence (FC) and backward convergence (BC) in the dimensionless translational speed / dimensionless lodging velocity plane are identified.

- The combined model is then used to carry out a sensitivity analysis to determine which crop parameters most affect the width of field lodged. The most important parameters are shown to be stem strength, stem radius, and overall plant drag area. However it is unlikely that breeding for specific

characteristics would result in crops that would be able to withstand tornado wind speeds without lodging.

- The combined model also allows a risk analysis of the lodging process to be carried out and it is shown that PDFs and CDFs of lodging width can be determined where the crop and tornado parameters are considered as stochastic variables.

- The variation of lodging width with maximum tornado speed can be determined from this risk analysis, and it shows that, if the crop parameters are known, then the lodging width allows an estimate of the maximum tornado velocity to be obtained.

Further work is still required in two areas.

- Fieldwork is required to determine lodging directions and lodging width around the tornado track, perhaps from aerial or satellite imagery, and also to determine the physical parameters of the crop (stem strength, radius and thickness and natural frequency) to enable more accurate determination of stem lodging velocities.

- If the spatial distribution of crops could be determined for any one particular region or country, and more information was available on lodging track lengths and the spatial distribution of plant characteristics, then the application of this methodology would allow probability distributions of total lodged area in any region or country to be calculated.

- The tornado model used in this paper also has the potential to be developed to investigate tree fall and damage on objects close to the ground, in the tornado boundary layer, where the flow changes from being wholly radial to having both radial and circumferential components.

References

Baker, C. J (1995) The development of a theoretical model for the windthrow of plants. Journal of Theoretical Biology, 175, 355-372

Baker, C.J., Sterling, M (2017) Modelling wind fields and debris flight in tornadoes, Journal of Wind Engineering and Industrial Aerodynamics 168, 312-321 http://dx.doi.org/10.1016/j.jweia.2017.06.017

Baker, C. J., Sterling, M (2018a) A conceptual model for wind and debris impact loading of structures due to tornadoes, Journal of Wind Engineering and Industrial Aerodynamics. 175, 283-291, https://doi.org/10.1016/j.jweia.2017.11.029 SEP

Baker, C. J., Sterling, M (2018b) The calculation of train stability in tornado winds, Journal of Wind Engineering and Industrial Aerodynamics. 176, 158-165, https://doi.org/10.1016/j.jweia.2018.03.022

Baker, C. J M Sterling , P M Berry (2014) "A generalised model of crop lodging", Journal of Theoretical Biology 363, 1–12 , http://dx.doi.org/10.1016./j.jtbi.2014.07.032

Berry, P. M (1998) Predicting lodging in winter wheat. PhD thesis. University of Nottingham. UK

Berry P, Sterling M, Baker C, Spink J, Sparks D (2003) "A calibrated model of wheat lodging compared with field measurements", Agricultural and Forest Meteorology, 119,167-180, http://dx.doi.org/10.1016/S0168-1923(03)00139-4

Berry P, M., Sterling M, Spink J, Baker C, Sylvester-Bradley R, Tams A, Ennos A (2004) "Understanding and reducing lodging in cereals", Advances in Agronomy 84, 217-269, http://dx.doi.org/10.1016/S0065-2113(04)84005-7

Berry, P.M (2019). Personal communication.

Chen G, Lombardo F (2019) "An analytical pattern-based method for estimation of a near-surface tornadic wind field", Journal of Wind Engineering and Industrial Aerodynamics 104, 103999,

https://doi.org/10.1016/j.jweia.2019.103999

Dotzeka, N, Grieser, J, Brooks, H (2003) "Statistical modeling of tornado intensity distributions", Atmospheric Research 67–68, 163–187,

http://dx.doi.org/10.1016/S0169-8095(03)00050-4

Fan F, Pang, W (2019) Stochastic Track Model for Tornado Risk Assessment in the U.S.", Frontiers of the Built Environment,

https://doi.org/10.3389/fbuil.2019.00037

Fischer, R. A., and Stapper, M. (1987). Lodging effects on high yielding crops of irrigated semidwarf wheat. Field Crops Research. 17, 245–248.

Forbes, G. S and Wakimoto, R. M. (1982) A concentrated outbreak of tornadoes, downbursts and microburst, and implications regarding vortex classification. Monthly Weather Review, Vol. 111, 220 – 235).

Haan, F, Sarkara, P, Gallus, W (2008) "Design, construction and performance of a large tornado simulator for wind engineering applications", Engineering Structures 30,1146–1159, https://doi.org/10.1016/j.engstruct.2007.07.010

Holland A, Riordan A, Franklin E (2006) "A simple model for simulating tornado damage in forests", Journal of Applied Meteorology and Climatology 45, 1597-1611,

Karstens C., Samaras T., Lee B., Gallus W. (2010) "Near gound pressure and wind measurements in tornadoes", Monthly Weather Review 138 (7), 2570-2588,

https://doi.org/10.1175/2010MWR3201.1.s1

Karstens C, Gallus W, Lee, B, Finley C (2013) "Analysis of Tornado-Induced Tree Fall Using Aerial Photography from the Joplin, Missouri, and Tuscaloosa–Birmingham, Alabama, Tornadoes of 2011", Journal of Applied Meteorology and Climatology 52, 1049- 1068, https://doi.org/10.1175/JAMC-D-12-0206.1

K.A. Kosiba and J. Wurman, (2013) The Three-Dimensional Structure and Evolution of a Tornado Boundary Layer, Weather Forecasting, 28, 1552–1561, https://doi.org/10.1175/WAF-D-13-00070.1

Lee W-C, Wurman J (2005) "Diagnosed Three-Dimensional Axisymmetric Structure of the Mulhall Tornado on 3 May 1999", Journal of the Atmospheric Sciences 62, 2373-2393, https://doi.org/10.1175/JAS3489.1

Lomardo F, Roueche D, Prevatt D (2015) "Comparison of two methods of near-surface wind speed estimation in the 22 May, 2011 Joplin, Missouri Tornado", Journal of Wind Engineering and Industrial Aerodynamics 138, 87-97, http://dx.doi.org/10.1016/j.jweia.2014.12.007

National Weather Service (2016) "How Many Tornadoes Can One Squall Line Produce?", https://nws.weather.gov/blog/nwsdesmoines/2016/08/06/

National Weather Service (2018a) "Rantoul Tornado", https://www.weather.gov/ilx/26June18GiffordRantoulTornado

National Weather Service (2018b) "Bondurant Tornado" https://www.weather.gov/dmx/20180719_Tornadoes

Neenan, M., and J. L. Spencer-Smith, 1975: An analysis of the problem of lodging with particular reference to wheat and barley. J. Agric. Sci. Cambridge 85, 494—507.

Pinthus, M. J., 1973: Lodging in wheat, barley and oats: the phenomenon, its causes and preventative measures. Adv. Agron. 25, 209—263.

Rhee D, Lomardo F (2018) "Improved near-surface wind speed characterization using damage patterns", Journal of Wind Engineering and Industrial Aerodynamics 180, 288-297, https://doi.org/10.1016/j.jweia.2018.07.017

Sterling, M., Baker, C. J., Berry, P. M., and Wade, A. (2003). An experimental investigation of the lodging of wheat. Journal of Agricultural and Forest Meteorology. Vol. 119, Issues 3 –4, 149 – 165.

Sterling M, Baker C, Joseph G, Gillmeier S, Mohammadi M, Blackburn G, Wyatt D, Gullick D, Berry P, Hatley D, Spink J, Finan J, Miao Y, Thanda D, Sonder K (2018) "Mitigating yield losses due to lodging of cereal crops", International Workshop on Wind-Related Disasters and Mitigation, Tohoku University, Sendai, Japan

Thomas, W. D. (1982). "Plant Growth Regulators". Yield of Cereals Course Papers, 1982. NAC Cereal Unit, RASE, Stoneleigh, UK, pp. 78–95.

White, E. M. (1991). Response of winter barley culivars to nitrogen and a plant growth regulator in relation to lodging. J. Agric. Sci. Cambridge 116, 191–200.
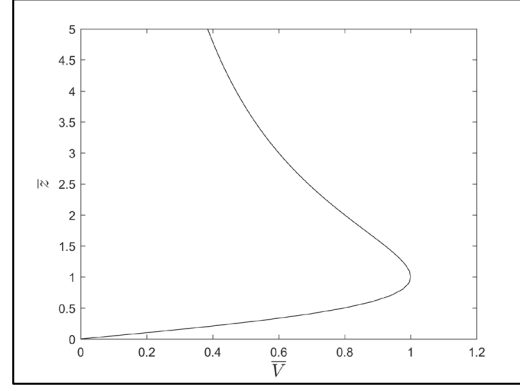
Appendix 1. The tornado model

The model outlined in Baker and Sterling (2017) begins with a realistic assumption of the radial velocity, and then obtains the vertical velocity distribution through the continuity equation, and the circumferential velocity and pressure through the momentum equations. In this note we take a different approach – beginning with a realistic circumferential velocity distribution and then calculating the vertical and radial velocities and pressures. The basic circumferential velocity assumption is

$$\bar{V} = \frac{4\bar{r}\bar{z}}{(1+\bar{r}^2)(1+\bar{z}^2)}$$
(A1.1)

where $\bar{V} = \frac{V}{V_m}$, $\bar{r} = \frac{r}{r_m}$ and $\bar{z} = \frac{z}{z_m}$. V, r and z are the circumferential velocity, radial distance from the vortex core and height above ground respectively, and V_m is the maximum value of V, which occurs at $r = r_m$ and $z = z_m$. The form assumed is very similar to that assumed for the *radial* velocity in Baker and Sterling (2017). The constant "four" in the numerator ensures that the $\bar{V} = 1$ when $\bar{r} = \bar{z} = 1$. The variation of $\bar{V}$ with $\bar{r}$ and $\bar{z}$ is shown in figure A1.1. The radial variation of the circumferential velocity thus takes the form similar to a Rankine vortex (i.e. proportional to radius for small $\bar{r}$ and inversely proportional to radius for large $\bar{r}$, with a maximum at $\bar{r} = 1$). The Rankine vortex model however is only concerned with the radial variation of circumferential velocity and does allow for a vertical variation. By contrast the current model assumes that the circumferential velocity increases from zero at the ground through a maximum at $\bar{z} = 1$ and then falling with increasing $\bar{z}$, in line with the experiments of Kosiba and Wurman (2013). The reduction in velocities near the ground in some ways models the viscous boundary layer that must exist beneath tornadoes at full scale.
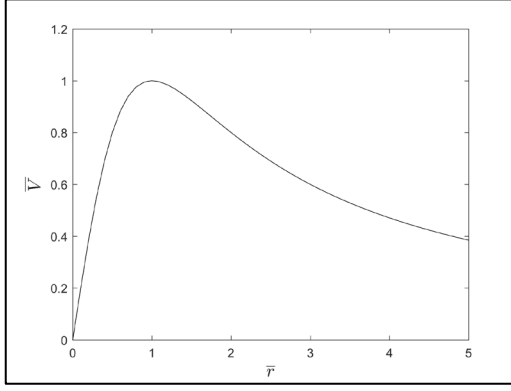
a) Variation of $\bar{V}$ with $\bar{r}$ for $\bar{z} = 1$ b) Variation of $\bar{V}$ with $\bar{z}$ for $\bar{r} = 1$

Figure A1.1 Assumed circumferential velocity distribution

Following the methodology adopted in the earlier work, the first step in the solution is to substitute the assumption of equation (A1.1) in the circumferential momentum equation

$$\bar{U}\frac{\partial \bar{V}}{\partial \bar{r}} + \frac{\bar{U}\bar{V}}{\bar{r}} + \frac{\bar{W}}{\delta}\frac{\partial \bar{V}}{\partial \bar{z}} = 0 \tag{A1.2}$$

where $\bar{U} = U/V_m$, $\bar{W} = W/V_m$ and $\delta = z_m/r_m$, where U is the radial velocity and W is the vertical velocity. This gives a relationship between $\bar{U}$ and $\bar{W}$ in terms of $\bar{r}$ and $\bar{z}$. We have a further relationship between $\bar{U}$ and $\bar{W}$ in the continuity equation

$$\frac{1}{\bar{r}}\frac{\partial(\bar{U}\bar{r})}{\partial \bar{r}} + \frac{1}{\delta}\frac{\partial \bar{W}}{\partial \bar{z}} = 0 \tag{A1.3}$$

and thus expressions for $\bar{U}$ and $\bar{W}$ can be found from these two relationships. This procedure is analytically quite complicated and requires the assumption that both $\bar{U}$ and $\bar{W}$ have the form $f(\bar{r})g(\bar{z})$, i.e. they are products of function of $\bar{r}$ and $\bar{z}$. The resulting velocity expression can then be used to find the pressure distribution using the radial momentum equation

$$\bar{U}\frac{\partial \bar{U}}{\partial \bar{r}} - \frac{\bar{V}^2}{\bar{r}} + \bar{W}\frac{\partial \bar{U}}{\partial \bar{z}} = -\frac{\partial \bar{P}}{\partial \bar{r}} \tag{A1.4}$$

where $\bar{P} = P/\rho V_m{}^2$ and P is the pressure and ρ is the air density.

Following this procedure results in the following expressions for dimensionless radial and vertical velocities

$$\bar{U} = -K \frac{\bar{r}^{\gamma-1}}{(1+\bar{r}^2)^{\gamma/2}} \frac{\bar{z}^{(\gamma-2)/2}(1-\bar{z}^2)}{(1+\bar{z}^2)^{(\gamma+2)/2}} \qquad (A1.5)$$

$$\bar{W} = \delta K \frac{2\bar{r}^{\gamma-2}}{(1+\bar{r}^2)^{(\gamma+2)/2}} \frac{\bar{z}^{\gamma/2}}{(1+\bar{z}^2)^{\gamma/2}} \qquad (A1.6)$$

Here K and γ are constants of integration, which are similar, but not identical to, those parameters with the same symbols in Baker and Sterling (2017). γ has a lower bound of 2.0 – below that the vertical velocity goes to infinity at the centre of the vortex. In what follows we will specifically consider the $\gamma = 2$ case, for which we obtain

$$\bar{U} = -K \frac{\bar{r}}{(1+\bar{r}^2)} \frac{(1-\bar{z}^2)}{(1+\bar{z}^2)^2} \qquad (A1.7)$$

$$\bar{W} = \delta K \frac{2}{(1+\bar{r}^2)^2} \frac{\bar{z}}{(1+\bar{z}^2)} \qquad (A1.8)$$

These profiles are plotted in figure A1.2 for $\bar{U}/K$ and $\bar{W}/K\delta$ in a vector plot format. The profiles show a classic updraft with a peak in the vertical velocity component at the vortex centre, but which falls in magnitude as $\bar{z}$ increases i.e. the vertical velocity is bounded, unlike the model of Baker ad Sterling (2017). There is a strong radial inflow at the lower heights, with a non-zero value at $\bar{z}=0$ that falls to zero at $\bar{z}=1$ and there is a weak outflow above this. This non-zero value of radial velocity at the ground is particularly useful for the application considered in this paper. This form is thus broadly consistent with the one-cell vortex observation at both full and model scale (see Haan et al., (2008) and Lee and Wurman (2005) for typical schematic sketches). The maximum value of radial velocity occurs at $\bar{r} = 1$ and $\bar{z} = 0$. Thus
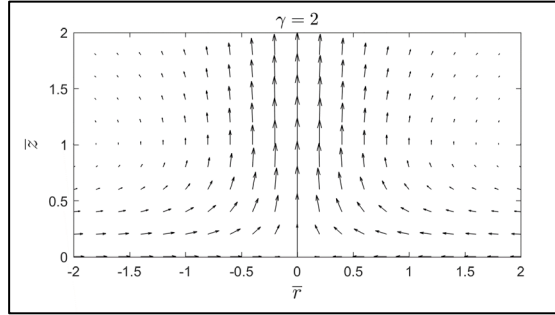
$$K = 2\frac{U_m}{V_m} \tag{A1.9}$$

Figure A1.2 Vector plot in $\bar{r}$ - $\bar{z}$ plane of $\overline{U}/K$ and $\overline{W}/K\delta$ for $\gamma = 2$

Finally, whilst only the $\gamma = 2$ case is considered here, it is worth noting that for higher values of γ the nature of the flow pattern changes, with vertical velocity peaks away from the vortex centre, and a form that approaches that of two cell vortices, although with no central downflow. This might be useful for other applications in the future.

Appendix 2 Further considerations of the tornado / lodging model

The tornado model outlined in Appendix 1 has been used in the main text for a dimensionless height $\bar{z}$ = 0 i.e. at ground level. Here the flow is completely radial in direction. However away from the ground the model displays, in addition, a circumferential component of velocity. It can be shown that the wind velocity and direction equations equivalent to equations (12) and (13) have the following, somewhat more complex form.

$$\bar{\Omega} = \left(\bar{Q}^2 + \frac{(\bar{x}^2+\bar{y}^2)\left(K^2(1-\bar{z}^2)^2+16\bar{z}^2(1+\bar{z}^2)^2\right)}{(1+\bar{x}^2+\bar{y}^2)^2(1+\bar{z}^2)^4} - \frac{2\bar{Q}\left(K(1-\bar{z}^2)\bar{x}+4\bar{z}(1+\bar{z}^2)\bar{y}\right)}{(1+\bar{x}^2+\bar{y}^2)(1+\bar{z}^2)^2} \right)^{0.5} \quad \text{(A2.1)}$$

$$\phi = atan\left(\frac{-K(1-\bar{z}^2)\bar{y}+4\bar{z}(1+\bar{z}^2)\bar{x}}{Q(1+\bar{x}^2+\bar{y}^2)(1+\bar{z}^2)^2-K(1-\bar{z}^2)\bar{x}+4\bar{z}(1+\bar{z}^2)\bar{y}} \right) \quad \text{(A2.2)}$$

At $\bar{z}$ = 0 these reduce to equations (12) and (13). At $\bar{z}$ = 1, the radial velocity component disappears and the equations simply represent a translating rotational flow.

Now, if we assume that lodging is due to the wind speed at a height $\bar{z}$ and that the crop lodges in the direction at the point where this wind speed exceeds the lodging wind speed, then lodging direction plots analogous to those of figures 3 can be constructed. These are shown in figure A2.1 below for a range of values of $\bar{z}$, for the base case parameters $\widetilde{\Omega}_L$ = 0.5 and $\widetilde{Q}$ = 0.15, to be consistent with figure 3. For $\bar{z}$ = 0 (figure 3d) and $\bar{z}$=0.05 (figure A2.1a), the lodging directions are of the forward convergence (FC) type, with a convergence on a lodging angle of 0°. Some slight asymmetry appears as $\bar{z}$ moves away from zero. For $\bar{z}$=0.25 (figure A2.1b), the flow is of an asymmetric backward convergence (BC) type, with a convergence on a lodging angle of ±180°, with the line of convergence in the positive $\bar{y}$ direction towards the edge of the lodging front At $\bar{z}$ = 0.5 (figure A2.1c) the degree of asymmetry has increased significantly. For $\bar{z}$ = 1 (figure A2.1d) the lodging

direction pattern has changed to what might be termed a vortex (V) pattern, with a significant component roughly normal to the tornado track, as might be expected from a strong vortex flow.

The degree of symmetry can be characterized by the parameter R where

$$R = \frac{\overline{\Delta}^*}{\overline{\Delta}} \qquad\qquad (A2.3)$$

where $\overline{\Delta}^*$ is the dimensionless lodging width between the convergence line and the positive edge of the lodging front, and $\overline{\Delta}$ is the overall dimensionless lodging width. For the symmetric case R=0.5. The variation of R with $\bar{z}$ is shown in figure A2.2 below, together with the boundaries of the different lodging regions.
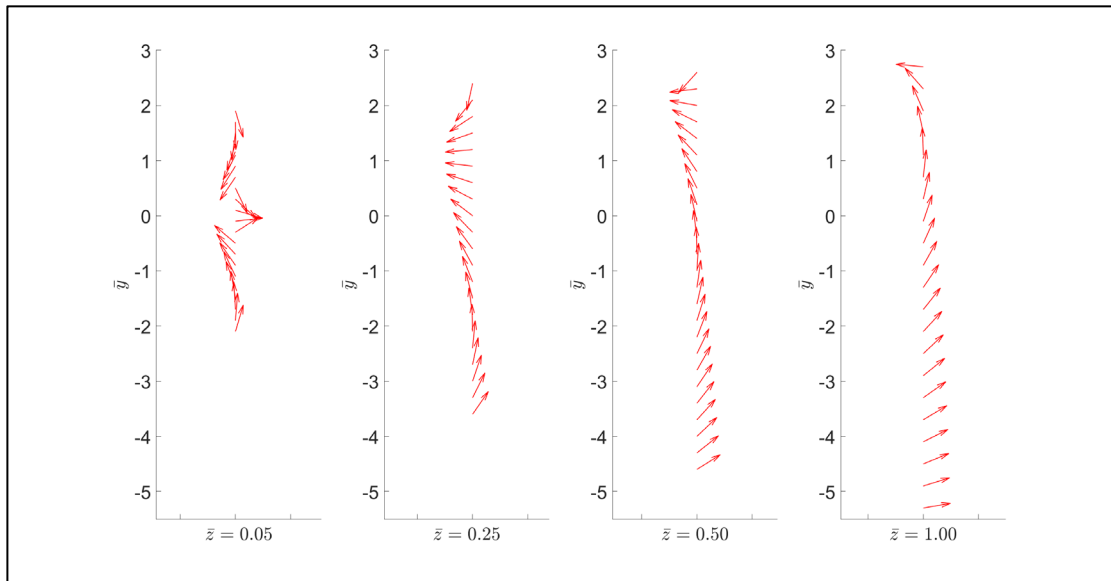

Figure A2.1 Variation of lodging direction with $\bar{z}$ for $\widetilde{\Omega}_L$ = 0.5 and $\widetilde{Q}$ = 0.15
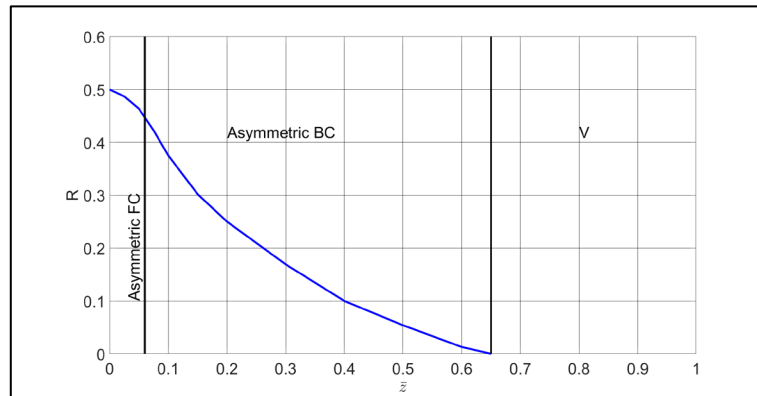
Figure A2.2 Degree of symmetry and regions of different lodging direction type